Available online at www.sciencedirect.com
ScienceDirect
Journal of Sound and Vibration 309 (2008) 150–166
JOURNAL OF SOUND AND VIBRATION
www.elsevier.com/locate/jsvi

Analytical evaluation in the design of a coating

G. Maidanik, L.J. Maga*

Carderock Division, Naval Surface Warfare Center, 9500 MacArthur Boulevard, West Bethesda, MD 20817-5700, USA

Received 19 December 2005; received in revised form 21 July 2006; accepted 7 June 2007

Abstract

The surface impedance of a coating is investigated and defined. The surface impedance is governed largely by the bulk modulus and the associated loss factor. The bulk modulus is but one of a number of moduli that characterize the properties of a coating. The bulk modulus and the shear modulus are the most commonly recognized. The normalized forms of the moduli are related by functions of Poisson's ratio. The normalization of a modulus is by the value of the modulus at the lowest frequency of interest. Were Poisson's ratio to be also independent of frequency, the normalized moduli, as functions of frequency, would all be identical. Since the loss factor that is associated with a normalized modulus is causal, when the normalized moduli are identical so are the associated loss factors. Were Poisson's ratio to be dependent on frequency, the normalized moduli, as functions of frequency, might be regionally or even universally different, and so would be the associated loss factors. Primitive descriptions of typical normalized moduli and the associated loss factors illustrate the design of a coating. The provided data set of the bulk and shear moduli of a coating are employed to test these analytical descriptions of the coating. Of particular interest in these tests is the causal relationship between a normalized modulus and the associated loss factor.
Published by Elsevier Ltd.

1. Introduction

Coatings are placed on wet surfaces to isolate them from the fluid in which they are immersed. A coating not only provides compliance, which is the mechanism that isolates, but it also provides a characteristic damping term. Occasionally, the damping that is contributed by the coating is crucial to its use. In this paper, a suggestion is made as to how to test cursorily the characteristics that control the mechanical properties of the coating and learn whether these characteristics admit to general design criteria. The tests are conducted so that if these design criteria are not met, the tests may reveal remedial measures. The simplicity inherent in these tests will further reveal whether these remedial measures may be implemented without reverting to radical design changes. Changes of this kind are both time consuming and costly.

A coating is largely characterized by the surface impedance that it contributes to the structure in which the coating is a component. A structure of this kind and the position of the coating therein are sketched in Fig. 1. Two variations on the theme, for such a structure and the coating that it accommodates, are sketched in Figs. 1a and b. The circuit diagrams for the analyses of these structures are presented in Figs. 2a and b,

*Corresponding author.
E-mail address: lawrence.maga@navy.mil (L.J. Maga).

0022-460X/$ - see front matter Published by Elsevier Ltd.
doi:10.1016/j.jsv.2007.06.076

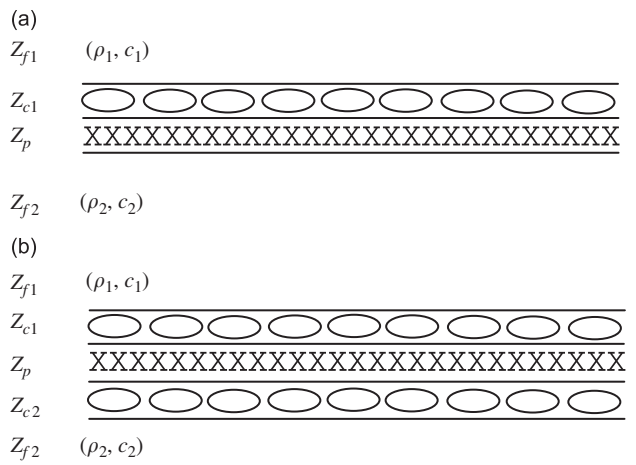

Fig. 1. Coated plate immersed in fluid media: Fluid no. 1 atop and fluid no. 2 at the bottom: (a) the coating is attached to a plate on one side and faces fluid no. 1 on the other, and (b) the coatings are attached to a plate on both sides; the top surface of the top coating faces fluid no. 1 and the bottom surface of the bottom coating faces fluid no. 2.

respectively. Using these circuit diagrams the analytical accountings may be derived. These derivations are presented in Table 1. Interest in this paper, however, is reserved largely for consideration and analysis of the surface impedance $z_c(k, \omega)$ of a coating, which may be cast in the form

$$Z_c(k,\omega) = (\mathrm{i}\omega)^{-1}[B(k,\omega)/t_c][1 + \mathrm{i}\eta_c(k,\omega)], \tag{1}$$

where (k, ω) is the spectral vector spanning the surface of the structure, k the wavevector and ω the frequency, t_c the thickness, $B(k, \omega)$ the bulk modulus and $\eta_c(k, \omega)$ the indigenous loss factor associated with this bulk modulus of the coating. The role that the coating plays as a component in a structural system; e.g., as depicted in Figs. 1 and 2, is considered under separate cover [1]. The parametric descriptions involved in Eq. (1) are lumped in a manner that renders Eq. (1) simple and algebraic. In the resulting equation, the dependence on the wavevector k is suppressed. The validity for this suppression requires the spatial variability in the coating to be small. If b denotes a typical spatial variability the suppression is validated provided $b|k| \ll 1$. Waves propagating in the coating then sense the coating to be spatially uniform. The result of this rendering is

$$Z_c(k,\omega) \Rightarrow Z_c(\omega) = (\mathrm{i}\omega)^{-1}[B(\omega)/t_c][1 + \mathrm{i}\eta_c(\omega)]. \tag{2a}$$

The properties of the coating, stated in Eq. (2a), are specified once the bulk modulus $B(\omega)$, the thickness t_c and the indigenous loss factor $\eta_c(\omega)$ are known. It is conducive to factorize the surface impedance $Z_c(\omega)$ of the coating in the form

$$\begin{aligned} Z_c(\omega) &= z_{c0}(\omega)\bar{B}(\omega)[1 + \mathrm{i}\eta_c(\omega)], \quad Z_{c0}(\omega) = (\mathrm{i}\omega)^{-1}(B_0/t_c), \\ \bar{B}(\omega) &= [B(\omega)/B_0], \quad [\partial(B_0)/\partial\omega] = 0, \end{aligned} \tag{2b}$$

where $\bar{B}(\omega)$ is the normalized bulk modulus $Z_{c0}(\omega)$ is the nondispersive factor and $\bar{B}(\omega)[1 + \mathrm{i}\eta_c(\omega)]$ is the dispersive factor in the surface impedance $Z_c(\omega)$ of the coating. The normalizing bulk modulus B_0 is the bulk modulus $B(\omega)$ at the lowest frequency of interest, which usually is a quiescent frequency region for $B(\omega)$. In the passive coating considered here the normalized bulk modulus $\bar{B}(\omega)$ is a monotonically increasing function of the normalized frequency ω, and therefore $\bar{B}(\omega) \Rightarrow 1$ as $\omega \Rightarrow 0$, where the normalizing frequency, designated by $(1/a)$, is yet to be judicially selected. It is established that there exists a relationship between the normalized bulk modulus $\bar{B}(\omega)$ and the associated loss factor $\eta_c(\omega)$. The relationship demands that $\eta_c(\omega)$ be causal to $\bar{B}(\omega)$ [2–5]. Thus, once the normalized bulk modulus $\bar{B}(\omega)$ is determined, the determination of the dispersive factor in $Z_c(\omega)$ follows.

A coating, in general, is a multimoduli structure of which the normalized bulk modulus $\bar{B}(\omega)$ and the associated loss factor $\eta_c(\omega)$ are more directly involved in isolating a surface from its fluid environment

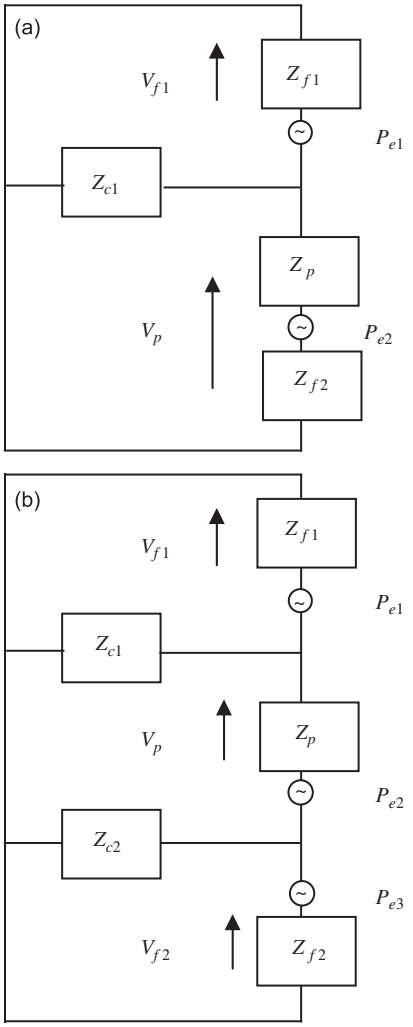

Fig. 2. Circuit diagram representations of: (a) Fig. 1a and (b) Fig. 1b.

Table 1
Surface impedance analyses of the dynamic systems: (a) the dynamic system described in Figs. 1a and 2a and (b) the dynamic system described in Figs. 1b and 2b

(a)
$$\begin{pmatrix} Z_{f1}+Z_{c1} & -Z_{c1} \\ -Z_{c1} & Z_{c1}+Z_p+Z_{f2} \end{pmatrix} \begin{pmatrix} V_{f1} \\ V_p \end{pmatrix} = \begin{pmatrix} P_{e1} \\ P_{e2} \end{pmatrix}$$

(b)
$$\begin{pmatrix} (Z_{f1}+Z_{c1}) & -Z_{c1} & 0 \\ -Z_{c1} & (Z_{c1}+Z_p+Z_{c2}) & -Z_{c2} \\ 0 & -Z_{c2} & Z_{c2}+Z_{f2} \end{pmatrix} \begin{pmatrix} V_{f1} \\ V_p \\ V_{f2} \end{pmatrix} = \begin{pmatrix} P_{e1} \\ P_{e2} \\ P_{e3} \end{pmatrix}$$

[cf. Figs. 1a and b]. In that sense, the normalized bulk modulus is often the prime target of the design. It is speculated that the normalized shear modulus $\bar{G}(\omega)$ and the associated loss factor $\eta_s(\omega)$ in the coating are responsible for providing the damping that the coating avails to the surface of the plating to which it is firmly attached. Again, $\eta_s(\omega)$ is causal to $\bar{G}(\omega)$. For this reason, the normalized shear modulus is also of significance

in designing the properties of the coating. In this paper, a generalized normalized modulus $\bar{M}(\omega)$ and the associated loss factor $\eta(\omega)$ are considered and the properties of this generalized normalized modulus are investigated. Of particular interest in these properties is the causal relationship between the normalized modulus and the associated loss factor. The properties, it transpires, are readily particularized to a specific normalized modulus; e.g., either to the normalized bulk modulus $\bar{B}(\omega)$ or to the normalized shear modulus $\bar{G}(\omega)$. The dispersive factor of a generalized surface impedance $\bar{M}(\omega)[1+i\eta(\omega)]$ is on hand once the normalized modulus $\bar{M}(\omega)$ is known, since the associated loss factor $\eta(\omega)$ is causal to $\bar{M}(\omega)$. There is still left open the question as to how do other normalized moduli and their associated loss factors, except for the bulk and the shear, contribute to the function of a multimoduli structure. Answering this question may beneficially render the coating multifunctional. This paper may even be the first step in this endeavor.

2. Normalized modulus in a coating

The description of a normalized form for a generalized lumped modulus $\bar{M}(\omega)$ in a multimoduli coating yields a ratio of rational functions, namely

$$\bar{M}(\omega)=\left[1+\sum_{n}^{N}\alpha_n(a\omega)^{n+\alpha}\right]\left[1+\sum_{h}^{H}\beta_h(a\omega)^{h+\beta}\right]^{-1},$$
$$\bar{M}(a\omega)=1 \quad \text{when } a\omega\Rightarrow 0, \tag{3}$$

where the α_n's, β_h's, N, H, α, β and a are the design parameters. It is to be understood that the n's and the h's are integers; e.g., $n=0, 1, 2, \ldots, N$ and $h=0, 1, 2, \ldots, H$ and that α and β are constants, which are not necessarily integers and are usually confined in the range $0\leqslant\alpha,\ \beta<1$. The parameter $1/a$ is a normalizing frequency, which, as already indicated, is yet to be appropriately selected. Eq. (3) may, thus, in general be quite elaborate. Although this elaboration may occasionally be called upon, it is rarely required in practice. Often drastic approximations suffice. Typical approximations of this kind merely require one term in the summations in Eq. (3) and, most often than not, β and h may be set equal to (α) and (n), respectively; $\beta=\alpha$, $h=n$, and β_n may be conveniently set equal to unity; $\beta_n=1$, so that Eq. (3) becomes

$$\bar{M}(\omega)=[1+\alpha_n(a\omega)^{n+\alpha}][1+(a\omega)^{n+\alpha}]^{-1}. \tag{4}$$

In Eq. (4), (α_n) is conditioned to exceed unity; $\alpha_n>1$, and this equation is dubbed primitive. In the primitive equation, $\bar{M}(\omega)$ starts at unity for $(a\omega)\Rightarrow 0$ and asymptotes to the value of (α_n) as $(a\omega)\Rightarrow\infty$. This characteristic often imitates those of many a practical normalized moduli. In the development of procedures for testing the viability of the designs for coatings one may employ equations that are similar to the primitive equations, à la Eq. (4). In circumstances in which design consideration exceeds those provided by the likes of Eq. (4), a few more elements in Eq. (3) may become mandatory. Analytical procedures in these circumstances follow, nonetheless, similar lines to those developed for the likes of Eq. (4).

One recognizes that Eq. (4) engrosses three design parameters: (1) the range parameter (α_n), (2) the power index ($n+\alpha$) and (3) the normalizing frequency parameter ($1/a$). The second of Eq. (3) reveals a silent design parameter. This additional parameter is $M_0=M(\omega)$ when $a\omega\Rightarrow 0$. The quantity M_0 is the normalizing modulus for $M(\omega)$; $\bar{M}(\omega)=[M(\omega)/M_0]$. It is convenient to replace the parameter $1/a$ by an appropriately selected normalizing frequency ω_M. This replacement will set a to be unity and will conveniently render the variable ω in Eq. (4) normalized.

3. Frequency normalization

There are a number of suitable normalizations of the frequency variable in the normalized modulus $\bar{M}(\omega)$, each of them with its own advantage and convenience. Without delving presently into the reasons for selecting the frequency normalization, it is, at this stage, merely stated that the value of the design frequency parameter ($1/a$) is selected to be the normalizing frequency (ω_M) that yields

$$\{\partial\ln[\bar{M}(\omega)]/\partial\omega\}=R(\omega); \quad \{\partial[\omega R(\omega)]/\partial\omega\}(a\omega=1)=0. \tag{5}$$

Clearly, it is anticipated that $\omega R(\omega)$ as a function of (ω) harbors a peak at $(\omega/\omega_M) = 1$. From Eqs. (3) and (5), one derives

$$\sum_{n}^{N}(n+\alpha)\alpha_n(a\omega)^{n+\alpha}\left[(n+\alpha)+\sum_{j}^{N}(n-j)\alpha_j(a\omega)^{j+\alpha}\right]\left[1+\sum_{h}^{H}\beta_h(a\omega)^{h+\beta}\right]^2$$
$$-\sum_{h}^{H}(h+\beta)\beta_h(a\omega)^{h+\beta}\left[h+\sum_{i}^{H}(h-i)\beta_i(a\omega)^{i+\beta}\right]\left[1+\sum_{n}^{N}\alpha_n(a\omega)^{n+\alpha}\right]^2=\bar{R}(a\omega), \tag{6}$$

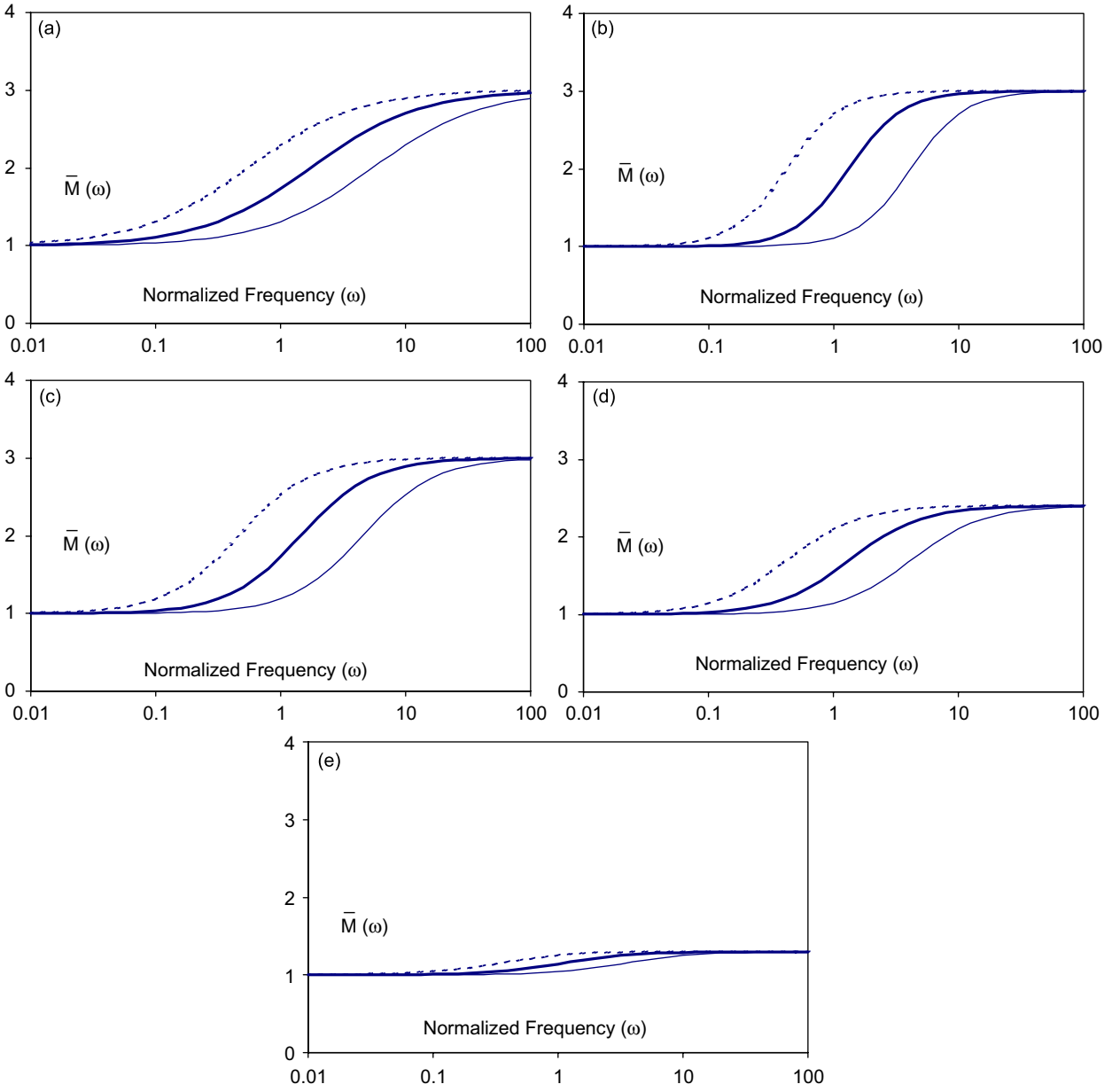

Fig. 3. Typical normalized modulus $\bar{M}(\omega)$ as a function of the normalized frequency (ω) for various range parameter (α_n) and power index $(n+\alpha)$ and the normalizing frequency (ω_M) [cf. Eqs. (8) and (9)]: (a) $(\alpha_1) = (3)$, $(n) = (1)$ and $(\alpha) = (0)$; (b) $(\alpha_2) = (3)$, $(n) = (2)$ and $(\alpha) = (0)$; (c) $(\alpha_1) = (3)$, $(n) = (1)$ and $(\alpha) = (1/2)$; (d) $(\alpha_1) = (2.4)$, $(n) = (1)$ and $(\alpha) = (1/2)$; and (e) $(\alpha_1) = (1.3)$, $(n) = (1)$ and $(\alpha) = (1/2)$.

where $\bar{R}(a\omega)$ is proportional to $\{\partial[\omega R(\omega)/\partial\omega]\}$. Were the normalizing frequency ω_M to be the frequency that maximizes $[\omega R(\omega)]$, it follows that

$$\bar{R}(a\omega_M) = 0. \tag{7}$$

Substituting the primitive Eq. (4) in Eq. (5) one derives

$$(\alpha_n)(a\omega_M)^{2n+2\alpha} = 1 \text{ or } a^n = [(\alpha_n)^{1/2}(\omega_M)^{n+\alpha}]^{-1}. \tag{8}$$

Eq. (4) may then be rewritten in the normalized frequency form

$$\begin{aligned} &\bar{M}(\omega) = [1 + (\alpha_n)^{1/2}\omega^{n+\alpha}][1 + (1/\alpha_n)^{1/2}\omega^{n+\alpha}]^{-1}, \\ &\bar{M}(\omega) \Rightarrow 1 \quad \text{when } (\omega) \ll 1 \quad \text{and} \quad \bar{M}(\omega) \Rightarrow \alpha_n \quad \text{when } (\omega) \gg 1, \end{aligned} \tag{9}$$

where in Eq. (9) ω is the normalized frequency variable; the frequency variable divided by the appropriate normalizing constant frequency ω_M.

The typical but primitive normalized modulus $\bar{M}(\omega)$, expressed in Eq. (9), is depicted by the bold solid curves, as a function of the normalized frequency, in Fig. 3. (The dashed and thin curves are reserved for the renormalization of the frequency, which is explained in Section 5.) Figs. 3a and b depict Eq. (9) with $\alpha = 0$, $\alpha_n = 3$, and $n = 1$ and 2, respectively. Fig. 3c depicts Eq. (9) with $\alpha = (1/2)$ and $\alpha_n = 3$ and $n = 1$. It is remarkable that these figures encompass the typical features exhibited by many of the normalized modulus $\bar{M}(\omega)$ in practical coatings designed for a variety of purposes. This statement becomes more obvious as further variations on the theme are exemplified. In this vein, Fig. 3c is repeated in Figs. 3d and e, respectively. In Figs. 3d and e, the standard value of (3) for the range parameter α_1 are changed, respectively, to (2.4) and (1.3). Again, the resemblance that the normalized moduli of many a coating bear to those presented in these figures is, remarkable. On those occasions when some elements in Eq. (3) need to be used to increase the matching, between the lumped description of a normalized modulus in an actual coating and that in a designed coating, the procedure is merely a slight tweak that results in the addition of a set of minor design parameters [cf. Appendix A].

4. Loss factor associated with a normalized modulus of a coating

In Eq. (2), the lumped loss factor $\eta_c(\omega)$ associated with the bulk modulus is introduced. It transpires that causality demands that this loss factor be related to the normalized bulk modulus $\bar{B}(\omega)$ [2–5]. Invoking causality through the Kramer–Kronig relationship, each loss factor $\eta(\omega)$ in the coating is thus associated with a corresponding normalized modulus $\bar{M}(\omega)$. This association is stated in the form

$$\eta(\omega) = (\pi\omega/4)R(\omega), \tag{10}$$

where $R(\omega)$ is defined in Eq. (5) and $\eta(\omega)$ is the loss factor that is associated with the normalized modulus $\bar{M}(\omega)$ in the coating. From Eq. (3) one obtains

$$\begin{aligned} \eta(\omega) = (\pi/4)\Bigg\{ &\sum_n^N (n+\alpha)\alpha_n(a\omega)^{n+\alpha}\left[1 + \sum_h^H \beta_h(a\omega)^{h+\beta}\right] \\ &- \sum_h^H (h+\beta)\beta_h(a\omega)^{h+\beta}\left[1 + \sum_n^N \alpha_n(a\omega)^{n+\alpha}\right]\Bigg\}^{-1} \\ &\times\left\{\left[1 + \sum_n^N \alpha_n(a\omega)^{n+\alpha}\right]\left[1 + \sum_h^H \beta_h(a\omega)^{h+\beta}\right]\right\}^{-1}. \end{aligned} \tag{11}$$

Further, if Eq. (4) is substituted for $\bar{M}(\omega)$, the result of this substitution yields the associated loss factor $\eta(\omega)$ in the primitive form

$$\eta(\omega) = [(n+\alpha)\pi/4](\alpha_n - 1)(a\omega)^{n+\alpha}\{[1 + \alpha_n(a\omega)^{n+\alpha}][1 + (a\omega)^{n+\alpha}]\}^{-1}. \tag{12}$$

Normalizing the frequency variable, à la Eqs. (7) and (8), one obtains

$$\eta(\omega) = [(n+\alpha)\pi/4][(\alpha_n)^{1/2} - (1/\alpha_n)^{1/2}]\omega^{n+\alpha}\{[1 + (\alpha_n)^{1/2}\omega^{n+\alpha}]\} \times [1 + (1/\alpha_n)^{1/2}\omega^{n+\alpha}]\}^{-1}. \tag{13}$$

In Eq. (13), as in Eq. (9), the frequency variable (ω) is connoted to be normalized by (ω_M).

The loss factor $\eta(\omega)$ stated in Eq. (13), is typically depicted by the bold solid curves, as a function of the normalized frequency, in Fig. 4. (Again, the dashed and thin curves are reserved for the renormalization of the frequency, which is explained in Section 5.) Figs. 4a–e pertain to the same parametric values that are employed in Figs. 3a–e, respectively. Therefore, for example, the loss factor $\eta(\omega)$ depicted in Fig. 4c pertains to the parametric values $(\alpha_1) = (3)$, $(n) = (1)$ and $(\alpha) = (1/2)$. These parametric values are used to depict Fig. 3c. As dictated by the second of Eq. (5) the maxima (peaks) in the primitive values of $\eta(\omega)$ occur on the normalized frequency axis, conveniently, at unity.

5. Frequency renormalizations

It is imperative that one recognizes that ω_M is merely a convenient substitution for $1/a$ in Eqs. (3), (4), (6), (11) and (12) and that $1/a$, or its equivalent (ω_M), is a design parameter in the coating. That equivalence is expressed in Eq. (7) and specifically for the primitive description of $\bar{M}(\omega)$ in Eq. (8). The normalizing frequency ω_M advantageously traces the peak value in the loss factor $\eta(\omega)$. Situations may arise in which the behavior of a dynamic system that incorporates the coating may conveniently demand a frequency normalization that is different from that of (ω_M). The normalizing frequency may then be changed to ω_0, say. This can be accomplished by replacing ω, which now stands for the frequency variable normalized by ω_0, by $s\omega$ in Eqs. (9) and (13), where $s = \omega_0/\omega_M$. This renormalization of the frequency variable merely amounts to a frequency shift. The shift is negative if $s>1$ and is positive if $s<1$. Shifts of this kind are depicted, for the normalized modulus $\bar{M}(\omega)$ and the associated loss factor $\eta(\omega)$, in Figs. 3a–e and in Figs. 4a–e, respectively. Negative shifts are indicated by the dashed curves and positive shifts by the thin curves.

6. The role of Poisson's ratio

It transpires that moduli in a coating are related to each other by Poisson's ratio (σ) [6]. This statement may be cast analytically in the form

$$M_1(\omega) = M(\omega)E_1(\sigma), \tag{14a}$$

where $E_1(\sigma)$ is a function of Poisson's ratio. For example, if $M_1(\omega)$ designates the shear modulus $G(\omega)$ and $M(\omega)$ the bulk modulus $B(\omega)$ then Eq. (14a) becomes

$$G(\omega) = B(\omega)E_G(\sigma); \quad E_G(\sigma) = [3(1-2\sigma)/2(1+\sigma)]. \tag{14b}$$

It follows that if (σ) is independent of the normalized frequency (ω), Eq. (14) may be restated in the normalized form

$$\bar{M}_1(\omega) = \bar{M}(\omega); \quad M_{10} = M_0E_1(\sigma), \tag{15a}$$

$$\bar{G}(\omega) = \bar{B}(\omega); \quad G_0 = B_0E_G(\sigma), \tag{15b}$$

where the zero-subscript designation is in reference to the moduli evaluated at a vanishing normalized frequency; $\omega \Rightarrow 0$. Also, as an example, for $\sigma = 13/30$ the value of $E_G(\sigma) \cong 0.14$ and, therefore, for a reasonable value of σ, $G_0 \ll B_0$. One may inquire whether Poisson's ratio, σ, is inherently independent of frequency or may there be circumstances when σ may be frequency dependent enough to cause a significant mismatch between $\bar{M}_1(\omega)$ and $\bar{M}(\omega)$; e.g., between $\bar{G}(\omega)$ and $\bar{B}(\omega)$. Even more intriguing is the question whether $\bar{M}_1(\omega)$; e.g., $\bar{G}(\omega)$ may, by design, be rendered significantly different from $\bar{M}(\omega)$; e.g., from $\bar{B}(\omega)$? With this difference the loss factors contributed by each may be made to peak at different frequencies enabling the manipulation of the indigenous damping contributed by the coating to be more versatile. At present, the answer to these questions remains, to the authors' knowledge, silent.

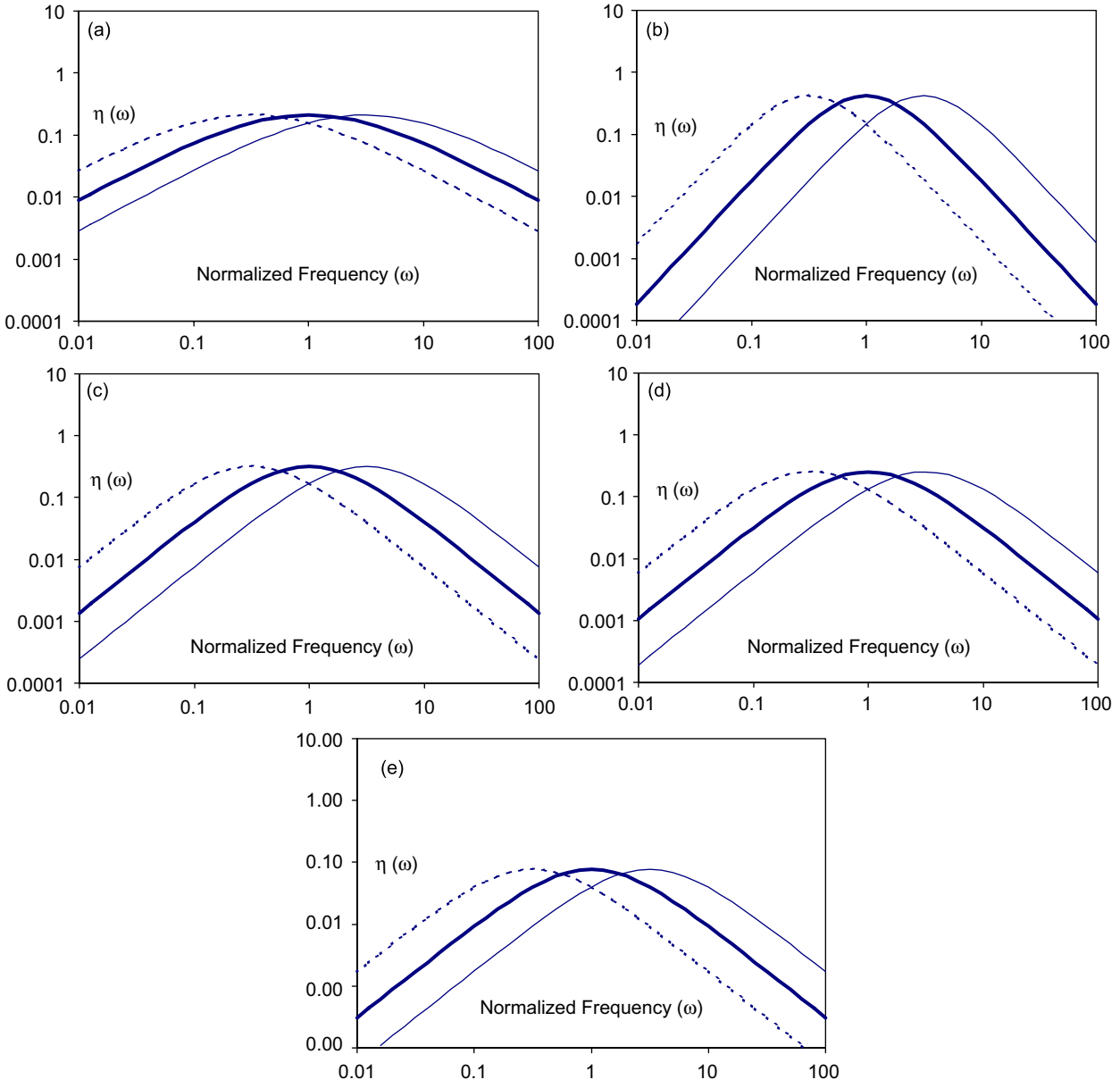

Fig. 4. The loss factor $\eta(\omega)$ that is associated with the normalized modulus $\bar{M}(\omega)$ as a function of the normalized frequency (ω) for various range parameter (α_n) and power index ($n+\alpha$): (a) $(\alpha_1)=(3)$, $(n)=(1)$ and $(\alpha)=(0)$ [cf. Fig. 3a]. (b) $(\alpha_2)=(3)$, $(n)=(2)$ and $(\alpha)=(0)$ [cf. Fig. 3b]. (c) $(\alpha_1)=(3)$, $(n)=(1)$ and $(\alpha)=(1/2)$ [cf. Fig. 3c]. (d) $(\alpha_1)=(2.4)$, $(n)=(1)$ and $(\alpha)=(1/2)$, [cf. Fig. 3d.] (e) $(\alpha_1)=(1.3)$, $(n)=(1)$ and $(\alpha)=(1/2)$ [cf. Fig. 3e].

7. Asymptotic evaluations of the normalized modulus and its

7.1. Associated loss factor

Focusing again on a typical normalized modulus $\bar{M}(\omega)$ one may inquire as to the sensitivity of this modulus and its associated loss factor $\eta(\omega)$ to the design parameters. The inquiry is partially answered by deriving the asymptotic evaluations of these two quantities. Using the primitive descriptions of $\bar{M}(\omega)$ and $\eta(\omega)$, as stated in

Eqs. (9) and (13), one derives

$$\bar{M}(\omega)=\begin{cases}1; & \omega^{n+\alpha}\ll(\alpha_n)^{-1/2},\\ (\alpha_n)^{1/2}; & \omega^{n+\alpha}=1,\\ (\alpha_n); & \omega^{n+\alpha}\gg(\alpha_n)^{1/2},\end{cases}\tag{16a–c}$$

$$\eta(\omega)=\begin{cases}[(n+\alpha)\pi/4][(\alpha_n)-1](1/\alpha_n)^{1/2}(\omega^{n+\alpha}); & \omega^{n+\alpha}\ll(\alpha_n)^{-1/2},\\ [(n+\alpha)\pi/4][(\alpha_n)-1][1+(\alpha_n)^{1/2}]^{-2}; & \omega^{n+\alpha}=1,\\ [(n+\alpha)\pi/4][(\alpha_n)-1](1/\alpha_n)^{1/2}(\omega^{n+\alpha})^{-1}; & \omega^{n+\alpha}\gg(\alpha_n)^{1/2}.\end{cases}\tag{17a–c}$$

The format of these equations; Eqs. (16) and (17), demonstrates that a typical normalized modulus $\bar{M}(\omega)$, as a function of the normalized frequency, is influenced largely by the values of the range parameter (α_n) rather than by the power index $(n+\alpha)$. The higher the values of (α_n) the higher the excursion of the normalized modulus from unity to higher values. The excursion extends over a larger frequency range the lower is the value of the power index $(n+\alpha)$ [cf. Figs. 3a–e]. On the other hand, a typical loss factor $\eta(\omega)$, as a function of the normalized frequency, is influenced largely by the value of the power index $(n+\alpha)$. The lower the values of $(n+\alpha)$ the more gentle is the decrease in the values of the loss factor as a function of the normalized frequency, away on either side of the peak in the loss factor [cf. Figs. 4a–e]. Nonetheless, it is imperative to understand that, both the values of $\bar{M}(\omega)$ and of $\eta(\omega)$, are determined by expressions that couple between the values of (α_n) and of $(n+\alpha)$; this coupling is essential in the design of the properties of the coating.

8. The so-called wicket plot

The practitioners who design and implement the coating often meet a dilemma. The dilemma is that the frequency characteristics of the coating; i.e., a typical normalized modulus $\bar{M}(\omega)$ and the associated loss factor $\eta(\omega)$, are functions of the frequency. The design of these two quantities as functions of the normalized frequency is central. It transpires that in the properties of a coating the temperature and the frequency are intimately related. Therefore, if the coating is to operate at different temperatures, there is a frequency shift that needs to be applied to determine the characteristics of the coating. Can some aspects of these characteristics of the coating be maintained independently of this shift? One aspect of this kind is afforded by the relationship that exists between the normalized modulus $\bar{M}(\omega);(\bar{M})=(M/M_0)$, and the associated loss factor $\eta(\omega)$ [cf. Eqs. (9) and (13)]. An advantage is taken of the fact that the normalized frequency variable ω can be eliminated in establishing a relationship between $\bar{M}$ and $\eta;\eta=\eta(\bar{M})$. Since this relationship is independent of frequency, it is also independent of the temperature. The display of $\eta=\eta(\bar{M})$ is known as the wicket plot [7].

In a coating that admits to a primitive description, the design of a typical normalized modulus requires merely the specification of three vocal parameters: The range parameter; e.g., α_n, the power index; e.g., $(n+\alpha)$ and the normalizing frequency; e.g., ω_M. In this coating, the relationship between the loss factor, η, and its normalized modulus $\bar{M}$; i.e., $\eta=\eta(\bar{M})$, is readily derived. Using Eqs. (9) and (13) one obtains

$$\eta(\bar{M})=[(n)+(\alpha)\pi/4](\bar{M}-1)[(\alpha_n)-\bar{M}]\{\bar{M}[(\alpha_n)-1\}^{-1}.\tag{18}$$

A number of asymptotic evaluations are in order

$$\eta\Rightarrow[(n+\alpha)\pi/4]\begin{cases}(\bar{M}-1); & 1<\bar{M}\Rightarrow 1,\\ [(\alpha_n)^{1/2}-1]^2[(\alpha_n)-1]^{-1}; & \bar{M}\Rightarrow(\alpha_n)^{1/2},\\ [1-(\bar{M}/\alpha_n)]; & (\alpha_n)>\bar{M}\Rightarrow(\alpha_n).\end{cases}\tag{19a–c}$$

[cf. Eqs. (16) and (17)]. The wicket plot of $\eta(\bar{M})$, as stated in Eq. (18), is illustrated in Fig. 5. In Fig. 5a, the relevant parameters are those employed in Figs. 3b and 4b. In Fig. 5b, the relevant parameters are $\alpha_1=2.4$, $n=1$ and $\alpha=0$ [cf. Figs. 3d and 4d]. Again, it is noted that the wicket plot for the coating that admits to a primitive description involves merely the range parameter α_n and the power index $(n+\alpha)$. However, there is an

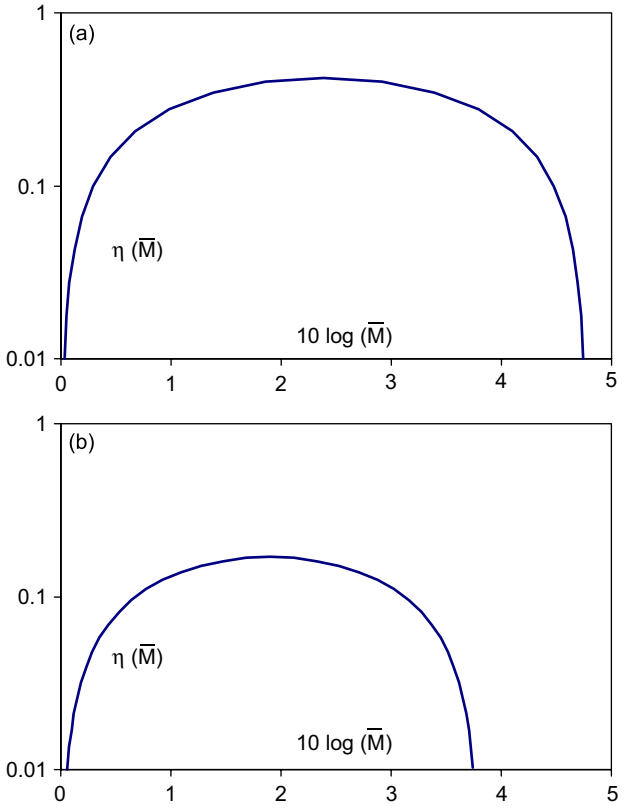

Fig. 5. The wicket plot of the loss factor $\eta(\bar{M})$ as a function of the normalized modulus $\bar{M}$; (η) is associated with the normalized modulus $(\bar{M})$. The wicket plot is presented for various range parameter (α_n) and power index (n), with $(\alpha)=0$: (a) $(\alpha_2)=(3)$ and $(n)=(2)$ [cf. Figs. 3b and 4b]; and (b) $(\alpha_1)=(2.4)$ and $(n)=(1)$.

oblique dependence on the range of $(\bar{M})$. This range is $1<\bar{M}<\alpha_n$. The left end limit of unity provokes the silent parameter M_0. The dependence of Eq. (18), as one may surmise, on the normalizing frequency ω_M is rendered moot. Clearly, the primitivism of the coating renders the relationship in the wicket plot simple. This simplicity is not an essential ingredient to its establishment. Were the description of the coating to be less primitive, the complexity of Eqs. (3), (6) and (11) could be used to establish the wicket plot nonetheless? However, consideration of this kind is outside the scope of this paper.

Acknowledgments

The authors are grateful to Dr. Jan Niemiec for helpful remarks, suggestions and guidance during the development and execution of this research work.

Appendix A. A case study of coating design

A case study is presented for which the designed or the measured data are provided; hereafter, referred to as the provided data. With respect to the coatings considered in the text, this case is an extreme. Moreover, the provided data of the bulk modulus exhibit, in the lower frequency range, a continued decrease with decrease in frequency. The study is undertaken to show that the primitive form of the analysis in the text can sustain these extremes. To account for the creep, in the lower frequency range, only a minor tweaking is subsequently introduced. The provided data covers about four (4) decades on the frequency axis, covering the frequency

range $10 \leqslant \omega/2\pi \leqslant 10^5$ Hz. These data relate to the two prime moduli in the coating: The bulk modulus $B(\omega)$ and the shear modulus $G(\omega)$. The provided data of $B(\omega)$ and of $G(\omega)$, on the same scale, is copied into Fig. A1a. As the text clarifies, the analysis that determines the loss factors that are associated with these moduli demands the normalized forms of these moduli. Preferably, but not imperatively, the normalizing moduli are those reached by the respective moduli at very low normalized frequencies; namely, $B_0 = B(\omega \ll 1)$ and $G_0 = G(\omega \ll 1)$, respectively. The frequencies at which the normalizing moduli are conveniently fixed are chosen to be equal. These normalizations yield

$$\bar{B}(\omega) = [B(\omega)/B_0]; \quad \bar{G}(\omega) = [G(\omega)/G_0]. \tag{A.1}$$

It was argued, in the text, that if Poisson's ratio (σ) is frequency independent then the normalized moduli are equal throughout the frequency range. The provided data show that

$$\bar{B}(\omega) = \bar{G}(\omega); \quad G_0/B_0 = 2 \times 10^{-3} \tag{A.2}$$

throughout the frequency range. The provided data for $\bar{B}(\omega)$ and $\bar{G}(\omega)$ are given in Fig. A1b. In this figure, the normalized moduli are expressed in terms of the normalized frequency (ω); the frequency is normalized by ω_M. The normalizing frequency (ω_M) is set to be $\omega_M/2\pi \cong 4.7 \times 10^4$ Hz and the normalized frequency covers the range $10^{-5} \leqslant \omega \leqslant 10^4$. Again, Poisson's ratio indeed appears to be independent of frequency in the entire

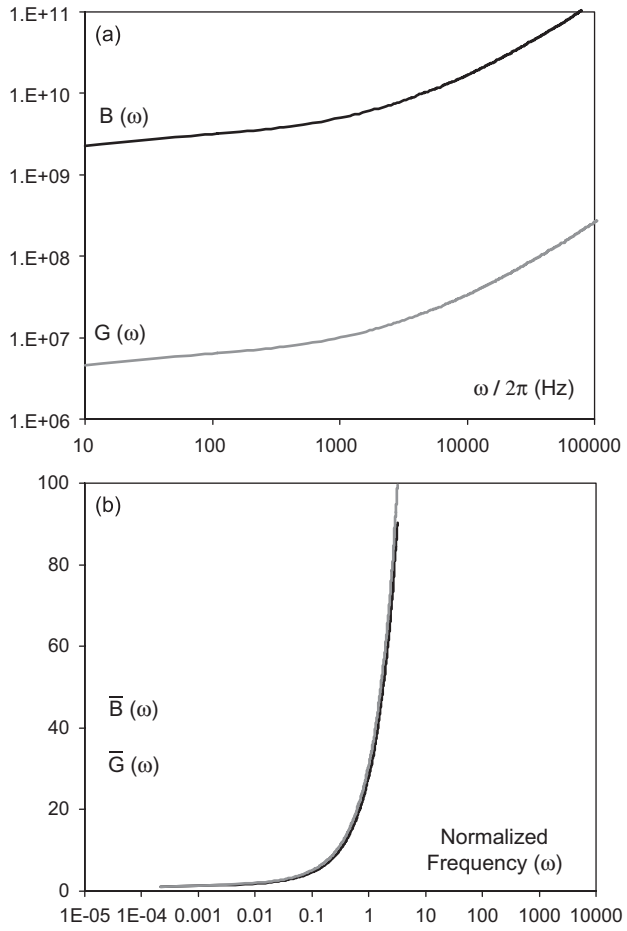

Fig. A1. The bulk modulus $B(\omega)$ and the shear modulus $G(\omega)$ as functions of the frequency (ω): (a) Neither the moduli nor the frequency are normalized, (b) both, the moduli and the frequency, are normalized. The normalizing moduli are (B_0) and (G_0), respectively, and the normalizing frequency is (ω_M) [cf. Eq. (7)].

normalized frequency range for which the provided data exist and, thus confirming, in this range, Eq. (A.2). This range spans $2.1 \times 10^{-4} < \omega < 2.1$. The validity of Eq. (A.2) is assumed herein and, therefore, it is sufficient to pursue one of these two normalized moduli, the second is a duplicate of the first. Using the primitive equation; Eq. (9), the normalized bulk modulus $\bar{B}(\omega)$ is computed as a function of the normalized frequency ω and the results are depicted in Fig. A2a. The vocal parameters; α_n, $(n+\alpha)$ and ω_M, in these computations are selected so that the computed data mimic the provided data where the latter are available. In this figure, the range parameter α_n is maintained at 830, the power index $(n+\alpha)$ is maintained at 1.08; $n = 1$ and $\alpha = 0.08$, and $\omega_M/2\pi = 4.7 \times 10^4$ Hz. The provided data are superposed on this figure for comparison purposes. Clearly, with the exception of the lower normalized frequency range the match is remarkable. The mismatch at the lower frequency range may be amplified by switching the ordinate scale from linear to log, as shown in Fig. A2b. An attempt to correct the mismatch reveals that a tweak may be required. Before tweaking, it may be of interest to continue the tweakless analysis. The primitive Eq. (13) is now employed to determine the loss factor $\eta_c(\omega)$ that is associated with the computed normalized modulus $\bar{B}(\omega)$ that is depicted in Fig. A2. The result of this determination is shown in Fig. A3. The provided data for $\eta_c(\omega)$ is superposed on this figure. The match between the computed data and the provided data is reasonable, but far from good. The matching fails even in those normalized frequency regions in which there exists a remarkably satisfactory matching between the computed and provide sets of data that pertain to the normalized modulus $\bar{B}(\omega)$; e.g., as depicted in Fig. A2 in the vicinity of unity for the normalized frequency ω. Since the computed loss factor $\eta_c(\omega)$ is causal

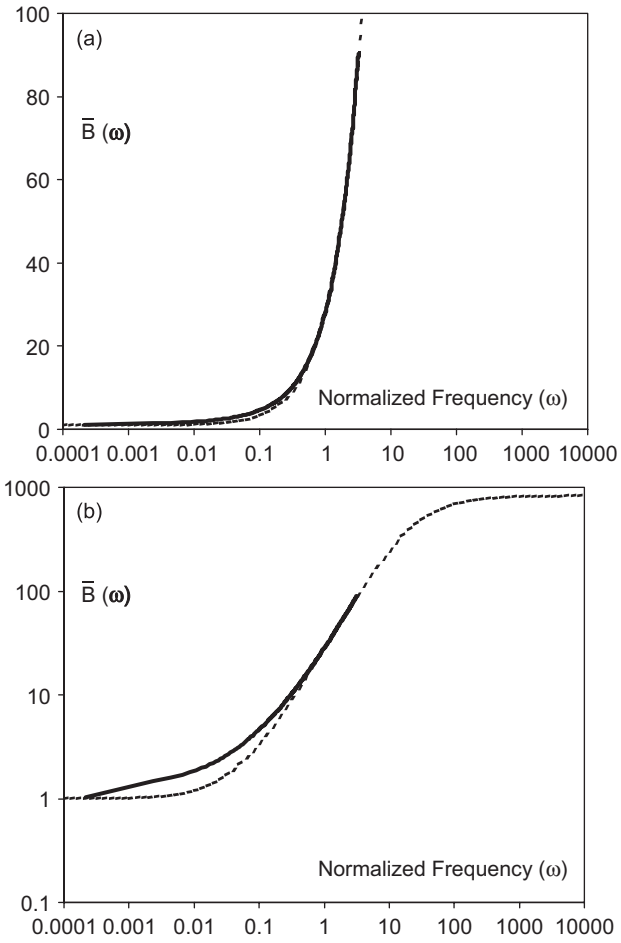

Fig. A2. Matching the computed data (dashed curve) with the provided data (solid curve) for the normalized bulk modulus $\bar{B}(\omega)$, as a function of the normalized frequency (ω). The computed data is derived of the primitive Eq. (9): (a) linear ordinate and (b) log ordinate.

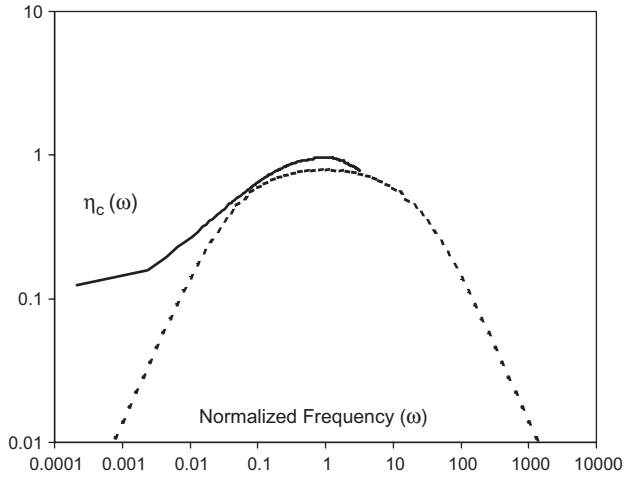

Fig. A3. Comparing the computed data (dashed curve) with the provided data (solid curve) for the loss factor $\eta_c(\omega)$ that is associated with the normalized bulk modulus $\bar{B}(\omega)$. The computed data is derived from the primitive Eq. (13).

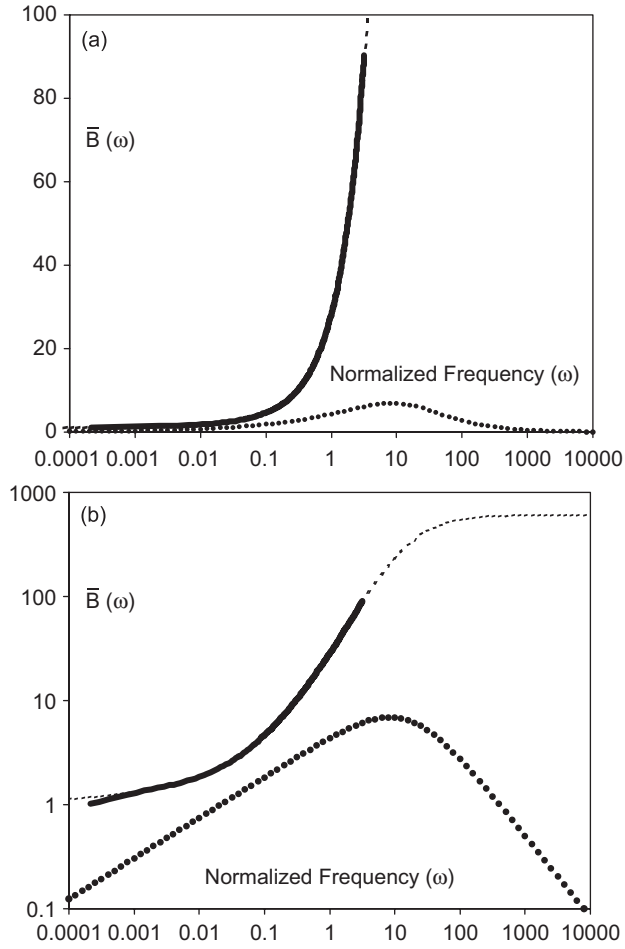

Fig. A4. Matching the computed data (dashed curve) with the provided data (solid curve) for the normalized bulk modulus $\bar{B}(\omega)$. The computed data is tweaked as specified in Eq. (A.3): (a) linear ordinate and (b) log ordinate.

to the associated $\bar{B}(\omega)$, does the provided data of the loss factor $\eta_c(\omega)$ reveal it to be noncausal to $\bar{B}(\omega)$? To answer this question more definitively an attempt is made to tweak the primitive Eq. (9) in order to achieve a better match between the computed data and the provided data with respect to the normalized bulk modulus $\bar{B}(\omega)$. Reference to Eqs. (3) and (8) suggest that a suitable tweak for $\bar{B}(\omega)$ in the lower frequency range would be of the form

$$\bar{B}(\omega) = [1 + (\alpha_n)^{1/2}\omega^{n+\alpha} + g_m^{n+\alpha}(\omega)][1 + (1/\alpha_n)^{1/2}\omega^{n+\alpha}]^{-1},$$
$$g_m^{n+\alpha}(\omega) = g\{(\alpha_n)^{1/2}\omega^{n+\alpha}\}^{(1/m)}, \tag{A.3}$$

where g and m are the minor design parameters in the presence of the vocal design parameters α_n, $(n+\alpha)$ and ω_M. With the tweak described in Eq. (A.3) the match between the computed data, based on this equation, and the provided data is shown in Fig. A4. The vocal parameters α_n, $(n+\alpha)$ and ω_M are selected to be $\alpha_n = 600$, $(n+\alpha) = 1.17$; $n = 1$ and $\alpha = (0.17)$, and $\omega_M/2\pi = 4.7 \times 10^4$ Hz and the tweak parameters (g) and (m) are selected to be $g = 1.55$ and $m = 3$. The match between the two data sets in Fig. A4 is remarkable throughout the frequency range for which the provided data are available. Again, in Fig. A4a the ordinate is chosen to be linear and in Fig. A4b it is log [cf. Fig. A2]. The causal loss factor $\eta_c(\omega)$ associated with the normalized bulk

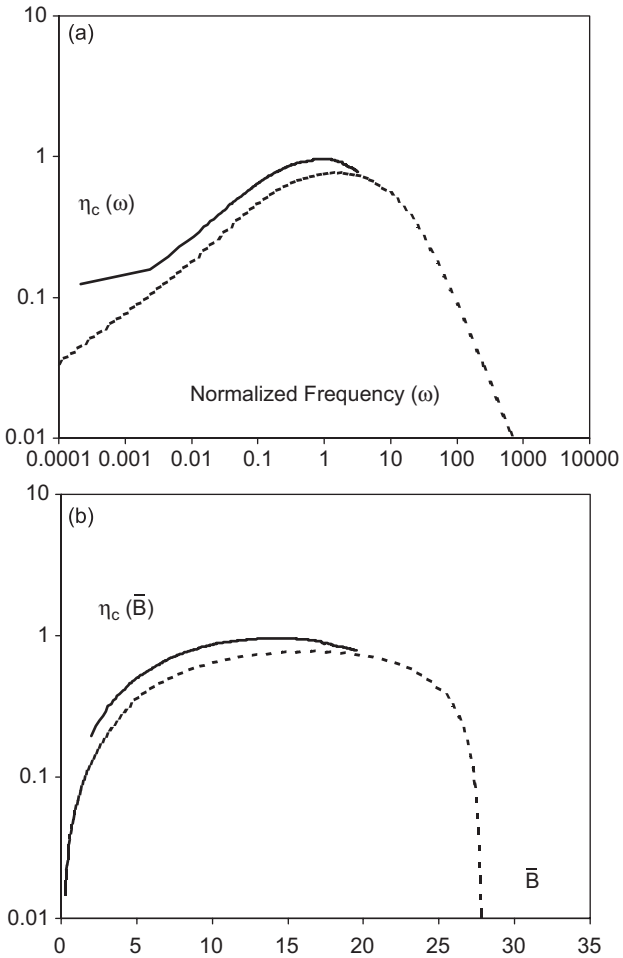

Fig. A5. Comparing the computed data (dashed curve) with the provided data (solid curve) for the loss factor $\eta_c(\omega)$ and the wicket plot that are associated with the normalized bulk modulus $\bar{B}(\omega)$. The computed data is derived of the causality of the tweaked normalized bulk modulus $\bar{B}(\omega)$, as specified in Eq. (A.3). The expression for the so computed loss factor is specified in Eq. (A.4): (a) the loss factor $\eta_c(\omega)$ as a function of the normalized frequency (ω) and (b) the loss factor $\eta_c(\bar{B})$ as a function of the normalized bulk modulus $(\bar{B})$.

modulus stated in Eq. (A.3) is derived to be

$$\eta_c(\omega) = [(n+\alpha)\pi/4]\{[(\alpha_n)^{1/2} - (1/\alpha_n)^{1/2}]\omega^{n+\alpha} + [g_m^{n+\alpha}(\omega)/m] \times [1 + (m-1)(1/\alpha_n)^{1/2}\omega^{n+\alpha}]\}/D_g(\omega),$$
$$D_g(\omega) = [1 + (\alpha_n)^{1/2}\omega^{n+\alpha} + g_m^{n+\alpha}(\omega)][1 + (1/\alpha_n)^{1/2}\omega^{n+\alpha}]. \quad (A.4)$$

Appropriately, when g is set equal to zero, Eqs. (A.3) and (A.4) reduce to Eqs. (9) and (13), respectively. Using Eq. (A.4) the loss factor $\eta_c(\omega)$ is computed, as a function of the normalized frequency (ω). Employing the parametric values used in the computation of $\bar{B}(\omega)$ depicted in Fig. A4, the computed data of the loss factor $\eta_c(\omega)$ are presented in Fig. A5a. The corresponding provided data for the loss factor $\eta_c(\omega)$ are superposed on Fig. A5a. Notwithstanding a different disposition, the matching between the two data sets in Fig. A5a is not improved over that presented in Fig. A3. The matching in Fig. A5a, however, could be significantly improved were the provided data treated to an octave up-shift in the normalized frequency as well as to an amplitude adjustment by a factor of (0.8). As Fig. A5b reveals this kind of improvement, between the computed data and the provided data, is available also for the corresponding wicket plot [7]. The provided data and the computed data, of $\bar{B}$ and of η_c to construct Fig. A5b are derived from Figs. A4 and A5a. In the wicket plot, naturally, the up-shift is in the value of the normalized bulk modulus $\bar{B}$ not in the normalized frequency (ω). Are these observations meaningful to the design of a coating? An oblique answer to the question may proceed as follows: A normalized modulus $\bar{M}$ is a fundamental characteristic of the coating; once it is specified and matched the coating is reasonably defined. On the other hand, stemming from the imposition of causality on that normalized modulus establishes the associated loss factor η. The authors are not privy to how the determination of the provided data of $\eta_c(\omega)$ were begot. However, once a match is established between the provided data and the computed data with respect to the normalized bulk modulus $\bar{B}(\omega)$ it follows that any discrepancy, between the provided data and the computed data with respect to the loss factor $\eta_c(\omega)$, is a violation of causality. A counter question then arises: Is causality a significant condition in the design of a coating? To appreciate the question just posed a twosome of figures is offered as closing remarks. The causality stated in Eq. (10) is performed on the provided data for the normalized bulk modulus $\bar{B}(\omega)$. This bulk modulus is exhibited in both in Figs. A2 and A4. The results of this causal performance are superposed on Fig. A5a to yield the first of the two figures; i.e., Fig. A6. Notwithstanding the granularity of the provided data of $\bar{B}(\omega)$, the causal results exhibited in Fig. A6 support the computed data rather than the corresponding provided data for the loss factor $\eta_c(\omega)$. In view of the match in Fig. A4, this is comforting, but

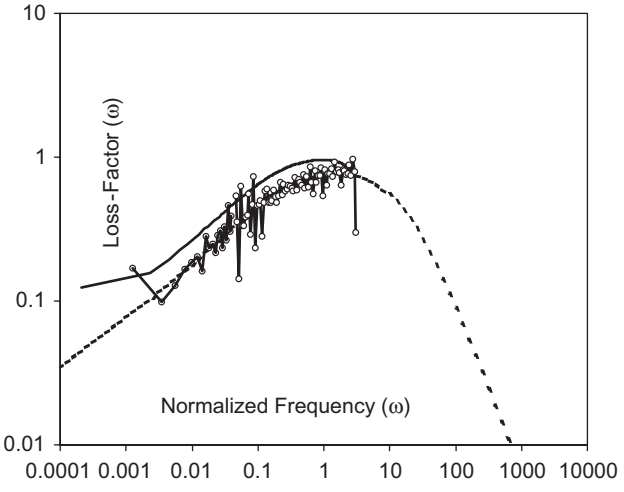

Fig. A6. Comparing the computed data (dashed curve) and the provided data (solid curve) for the loss factor $\eta_c(\omega)$ with the data (curve connecting open circles) derived for $\eta_c(\omega)$ on the basis of causality from the provided data for the normalized bulk modulus $\bar{B}(\omega)$. [The provided data for the normalized bulk modulus $\bar{B}(\omega)$ are depicted in Fig. A2 and also in Fig. A4.]

not surprising. In the second of the two figures; i.e., Fig. A7, the sensitivity of the computed normalized bulk modulus $\bar{B}(\omega)$ and its associated loss factor $\eta_c(\omega)$ to variations in the design parameters are examined. In Fig. A7a, the matched normalized bulk modulus $\bar{B}(\omega)$ that is depicted in Fig. A4b is compared with a slightly mismatched normalized bulk modulus. The mismatch in the two sets of computed data in Fig. A7a is introduced by slight modifications in the three design parameters that were central in the match with the provided data that is achieved in Fig. A4b. These modifications in the design parameters are the range parameter (α_n) is changed from (600) to (750), the power index ($n+\alpha$) is changed from (1.17) to (1.00) and the tweak parameter (g) is changed from (1.55) to (1.40). (Note that changing the power index from (1.17) to (1.00) amounts to setting $(\alpha)=(0)$ and $(n)=(1)$.) The influence of the mismatch on the normalized bulk modulus $\bar{B}(\omega)$ is shown in Fig. A7a. The influence of the mismatch on the associated loss factor $\eta_c(\omega)$ is shown in Fig. A7b. The disposition of the differences between the two sets of computed data in Fig. A7b is noncommittal. The situation in Fig. A7b is, however, more reminiscent of Fig. A3 than of Fig. A5a. In Fig. A3, the two sets of data are not reconcilable by either a shift in the normalized frequency, an amplitude adjustment or both. Yet, in Fig. A5a the two sets of data are reconcilable in that sense. Whether this feature in Fig. A5a is significant remains unanswered. Nonetheless, it emerges that to ascertain causally the associated loss factor $\eta(\omega)$ demands that knowledge, of the normalized modulus $\bar{M}(\omega)$ in the normalized frequency range of interest, be *a priori* minimally accurate.

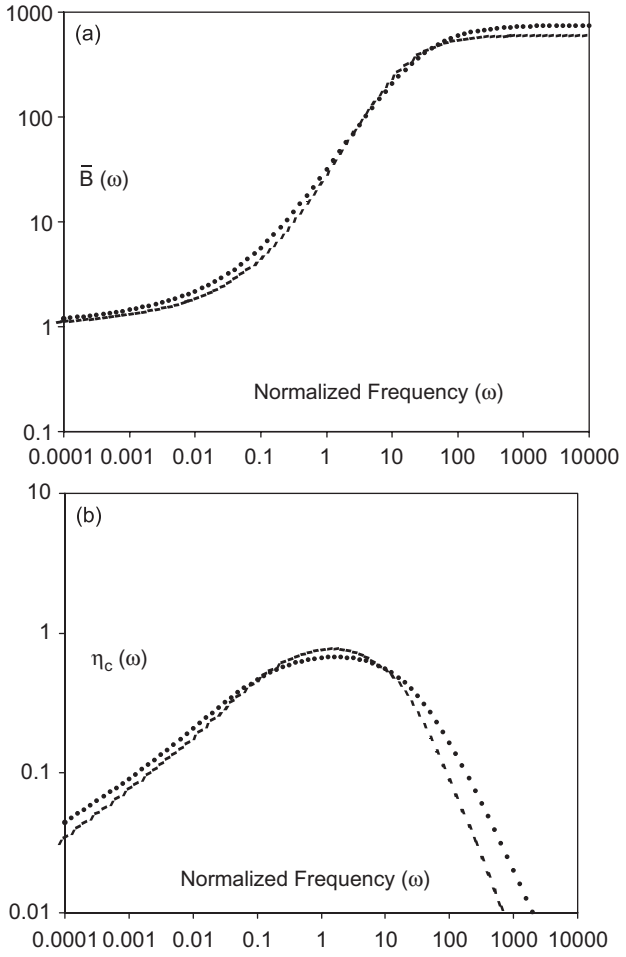

Fig. A7. A mismatched two sets of computed data for the normalized bulk modulus $\bar{B}(\omega)$. The mismatch is achieved by modifying some of the design parameters used in matching the provided data with the computed data in Fig. A4: (a) the mismatch in the normalized bulk modulus $\bar{B}(\omega)$, and (b) the corresponding mismatch in the associated loss factor $\eta_c(\omega)$.

References

[1] G. Maidanik, K.J. Becker, L.J. Maga, Dampings in naval coatings, Ship Signatures Department Technical Report, NSWCCD-70-TR–2005/127, November 2005.
[2] M. O'Donnell, E.T. Jaynes, J.G. Miller, Kramers–Kronig relationship between ultrasonic attenuation and phase velocity, *Journal of the Acoustical Society of America* 69 (1981) 696–701.
[3] M. O'Donnell, E.T. Jaynes, J.G. Miller, General relationship between ultrasonic attenuation and dispersion, *Journal of the Acoustical Society of America* 63 (1978) 1935–1937.
[4] T.M. Muller, B. Gurevich, Wave-induced fluid flow in random porous media: attenuation and dispersion of elastic waves, *Journal of the Acoustical Society of America* 117 (2005) 2732–2741.
[5] K. Aki, P.G. Richards, *Quantitative Seismology: Theory and Methods*, Freeman, New York, 1980.
[6] D. Ross, *Mechanics of Underwater Noise*, Pergamon, New York, 1976.
[7] W.M. Madigosky, G.F. Lee, J. Niemiec, A method for modeling polymer viscoelastic data and the temperature shift function, *Journal of the Acoustic Society of America* 119 (6) (June 2006).